



# Synergistic O<sub>3</sub> + OH oxidation pathway to extremely low-volatility dimers revealed in β-pinene secondary organic aerosol

Christopher M. Kenseth<sup>a</sup>, Yuanlong Huang<sup>b</sup>, Ran Zhao<sup>a</sup>, Nathan F. Dalleska<sup>b</sup>, J. Caleb Hethcox<sup>a</sup>, Brian M. Stoltz<sup>a</sup>, and John H. Seinfeld<sup>a,c,1</sup>

<sup>a</sup>Division of Chemistry and Chemical Engineering, California Institute of Technology, Pasadena, CA 91125; <sup>b</sup>Division of Geological and Planetary Sciences, California Institute of Technology, Pasadena, CA 91125; and <sup>c</sup>Division of Engineering and Applied Science, California Institute of Technology, Pasadena, CA 91125

Edited by Joost A. de Gouw, University of Colorado Boulder, Boulder, CO, and accepted by Editorial Board Member A. R. Ravishankara July 2, 2018 (received for review March 16, 2018)

Dimeric compounds contribute significantly to the formation and growth of atmospheric secondary organic aerosol (SOA) derived from monoterpene oxidation. However, the mechanisms of dimer production, in particular the relevance of gas- vs. particle-phase chemistry, remain unclear. Here, through a combination of mass spectrometric, chromatographic, and synthetic techniques, we identify a suite of dimeric compounds (C<sub>15–19</sub>H<sub>24–32</sub>O<sub>5–11</sub>) formed from concerted O<sub>3</sub> and OH oxidation of β-pinene (i.e., accretion of O<sub>3</sub>- and OH-derived products/intermediates). These dimers account for an appreciable fraction (5.9–25.4%) of the β-pinene SOA mass and are designated as extremely low-volatility organic compounds. Certain dimers, characterized as covalent dimer esters, are conclusively shown to form through heterogeneous chemistry, while evidence of dimer production via gas-phase reactions is also presented. The formation of dimers through synergistic O<sub>3</sub> + OH oxidation represents a potentially significant, heretofore-unidentified source of low-volatility monoterpene SOA. This reactivity also suggests that the current treatment of SOA formation as a sum of products originating from the isolated oxidation of individual precursors fails to accurately reflect the complexity of oxidation pathways at play in the real atmosphere. Accounting for the role of synergistic oxidation in ambient SOA formation could help to resolve the discrepancy between the measured atmospheric burden of SOA and that predicted by regional air quality and global climate models.

secondary organic aerosol | synergistic oxidation | atmospheric accretion chemistry | dimer formation | monoterpenes

The oxidation of monoterpenes (C<sub>10</sub>H<sub>16</sub>) represents a substantial and well-established source of atmospheric secondary organic aerosol (SOA) (1, 2), which constitutes a dominant mass fraction (15–80%) of fine particulate matter (PM<sub>2.5</sub>) (3) and exerts large but uncertain effects on Earth's radiative balance (4) as well as adverse impacts on regional air quality and human health (5, 6). High-molecular-weight, low-volatility dimeric compounds have been identified as significant components of both ambient (7–11) and laboratory-derived (12–22) monoterpene SOA, and have been implicated as key players in new particle formation and growth (9–14, 23–26), particle viscosity (27), and cloud condensation nuclei (CCN) activity (8, 24, 26).

Accumulating studies of α-pinene SOA indicate that a vast majority of these dimers are formed only through O<sub>3</sub>- and not OH-initiated oxidation, despite the apparent monomeric building blocks being present in both oxidative systems (11–13). Particle-phase reactions of closed-shell monomers [e.g., aldol addition/condensation (15–18), (peroxy)hemiacetal/acetal formation (16, 21, 22), esterification (7, 18–21), and gem-diol formation (16, 17)] and gas-phase reactions involving early-stage oxidation products and/or reactive intermediates [e.g., stabilized Criegee intermediates (SCIs), carboxylic acids, and organic peroxy radicals (RO<sub>2</sub>) (9–14, 23–26)] have been advanced as possible dimer formation pathways. However, the mechanisms

underlying dimer production and the relative importance of gas- vs. particle-phase chemistry remain unresolved.

In this work, we investigate the formation, identity, and abundance of molecular products in SOA derived from the O<sub>3</sub>- and OH-initiated oxidation of β-pinene, the second-most-abundant monoterpene emitted to the atmosphere (global emissions estimated at 19 Tg y<sup>-1</sup>) (28). Through detailed chromatographic and mass spectrometric analysis, coupled with <sup>13</sup>C isotopic labeling and OH/SCI scavenging, we identify a reactive pathway to extremely low-volatility dimeric compounds in SOA formed from monoterpene ozonolysis involving reaction of O<sub>3</sub>-derived products/intermediates with those generated from oxidation by OH produced in situ via vinyl hydroperoxide (VHP) decomposition. We present evidence for formation of these dimers via both gas- and particle-phase processes, underscoring the complexity of atmospheric accretion chemistry. In establishing that O<sub>3</sub> and OH can act in concert to form nontrivial yields of dimeric SOA constituents, we highlight the potential significance of synergistic oxidation in ambient aerosol formation.

## Results and Discussion

**Dimers in β-Pinene SOA.** β-Pinene ozonolysis and photooxidation experiments were carried out in the Caltech dual 24 m<sup>3</sup> Teflon Environmental Chambers (CTEC) (*Materials and Methods*). A

### Significance

Secondary organic aerosol (SOA) is ubiquitous in the atmosphere and plays a pivotal role in climate, air quality, and health. Monoterpenes, emitted in large quantities from forested regions, are a dominant source of SOA globally, with dimers having been identified as key contributors to particle formation and growth. Here, we establish the role of concerted oxidation by O<sub>3</sub> and OH as a significant route to dimer formation in SOA generated from β-pinene, the second-most-abundant monoterpene emitted to the atmosphere. Production of this class of dimers is found to occur through both gas- and particle-phase processes. Dimer formation via synergistic O<sub>3</sub> + OH oxidation could represent an appreciable source of “missing” SOA not included in current atmospheric models.

Author contributions: C.M.K. designed research; C.M.K., Y.H., and R.Z. performed research; J.C.H. and B.M.S. contributed new reagents/analytic tools; C.M.K., Y.H., R.Z., and N.F.D. analyzed data; and C.M.K. and J.H.S. wrote the paper.

The authors declare no conflict of interest.

This article is a PNAS Direct Submission. J.A.d.G. is a guest editor invited by the Editorial Board.

Published under the PNAS license.

<sup>1</sup>To whom correspondence should be addressed. Email: seinfeld@caltech.edu.

This article contains supporting information online at [www.pnas.org/lookup/suppl/doi:10.1073/pnas.1804671115/-DCSupplemental](http://www.pnas.org/lookup/suppl/doi:10.1073/pnas.1804671115/-DCSupplemental).

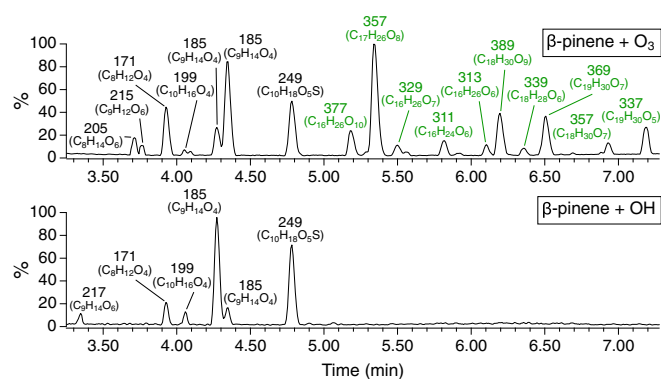


**Fig. 1.** UPLC(–)ESI-Q-TOF-MS BPI chromatograms of SOA produced from the  $O_3$ - and OH-initiated oxidation of  $\beta$ -pinene after  $\sim 4$  h of reaction in the CTEC (*SI Appendix, Table S1*, Exps. 1 and 2). Numbers correspond to nominal  $m/z$  values of  $[M-H]^-$  ions. Molecular formulas ( $C_xH_yO_z$ ) were assigned with mass tolerances of  $<7$  ppm and supported by associated  $^{13}C$  isotope distributions. Chromatograms consist of monomeric (black) and dimeric (green) regions.

custom-modified particle-into-liquid sampler (PILS) integrated with ultra-performance liquid chromatography/electrospray ionization quadrupole time-of-flight mass spectrometry operated in negative ion mode [UPLC(–)ESI-Q-TOF-MS] was used to characterize the time-resolved SOA molecular composition (*Materials and Methods*) (29). Base peak ion (BPI) chromatograms of the  $O_3$ - and OH-derived  $\beta$ -pinene SOA are shown in Fig. 1. The chromatographic fingerprint of the  $O_3$  system displays distinct monomeric and dimeric regions. Conversely, while the identities of the monomers in both systems are similar, dimers measurable by PILS + UPLC(–)ESI-Q-TOF-MS were not formed above the detection limit in the OH system, consistent with previous LC(–)ESI-MS studies on dimer formation in  $\alpha$ -pinene SOA (11–13). The monomers, on average, exhibit higher O:C ratios than the dimers, suggesting that deoxygenation (e.g., condensation) is operative in dimer formation (18, 21). That the dimers in the  $O_3$ -derived SOA elute at retention times (RT) distinct from those of the monomers and are undetected in SOA produced from OH oxidation demonstrates that they are authentic  $\beta$ -pinene SOA products rather than ion-source artifacts (e.g., noncovalent adducts) formed during the (–)ESI process.

The absence of detectable dimers in pinene photooxidation systems has prompted SCIs, specifically reaction of SCIs with first-generation carboxylic acids forming hydroperoxide esters (11, 12, 15), to be implicated as potential drivers of monoterpene accretion chemistry. However, we recently demonstrated that dimers identified in  $\alpha$ -pinene SOA using LC/ESI-MS methods do not contain (hydro)peroxide moieties (30). Further, no clear reduction in dimer abundance was observed for SOA generated from  $\beta$ -pinene ozonolysis when either water vapor or formic acid was introduced as an SCI scavenger (*SI Appendix, Fig. S1*). These findings, together with modest SCI yields (15%) measured for  $\alpha$ -pinene ozonolysis (31, 32), experimental and theoretical studies showing thermal unimolecular decay to be a dominant SCI loss process (32–34), and reported increases in dimer concentrations in  $\alpha$ -pinene SOA with increasing relative humidity (RH) (11–13) despite the probable role of water vapor as an SCI scavenger, call into question the importance of SCI chemistry in monoterpene dimer production. The lack of peroxide dimers in  $\alpha$ -pinene SOA also implies that gas-phase dimers formed via  $RO_2$  self/cross-reactions ( $RO_2 + RO_2 \rightarrow ROOR + O_2$ ) (23–26) do not retain their peroxide character (i.e., undergo chemical transformation/decomposition) following condensation to the particle phase, as previously suggested (13, 20, 23).

Although dimers in pinene SOA seem to form only through  $O_3$ - and not OH-initiated oxidation, scavenging of OH radicals produced as a byproduct of the hot Criegee VHP channel during  $\alpha$ -pinene ozonolysis has been found to suppress the formation of certain dimeric species (11). To further explore this effect,

steady-state  $\beta$ -pinene ozonolysis experiments were conducted in the Caltech Photooxidation Flow Tube (CPOT) in the presence and absence of cyclohexane as an OH scavenger (*Materials and Methods*). UPLC(–)ESI-Q-TOF-MS was employed to measure the molecular composition of SOA samples collected on Teflon filters and extracted into  $H_2O$  (*Materials and Methods*). A group of 23 dimeric compounds, also present in the CTEC experiments, was identified whose formation was significantly inhibited ( $>65\%$ ) by introduction of the OH scavenger; four of the dimers are major peaks in the BPI chromatogram (Fig. 2). These dimers, with molecular formulas  $C_{15-19}H_{24-32}O_{5-11}$  and O:C ratios ranging from 0.26 to 0.61, exhibit saturation mass concentrations ( $C^*$ )  $< 3 \times 10^{-4} \mu g m^{-3}$  and are designated as extremely low-volatility organic compounds (ELVOC) (Table 1). Compounds with accurate masses/molecular formulas corresponding to 20 of the 23 identified dimers have been measured in recent monoterpene SOA formation experiments, and 18 such compounds have been observed in ambient SOA samples from forested regions dominated by monoterpene emissions (*SI Appendix, Table S2*). The clear conclusion from these experiments is that formation for this particular collection of dimeric species depends on both  $O_3$  and OH oxidation, in either a concurrent or sequential manner.

**Dimers from Ozonolysis of  $^{13}C$ - $\beta$ -Pinene.** To determine the point in the  $O_3$ -initiated dimer formation pathway at which OH radical chemistry occurs (e.g., oxidation of the precursor hydrocarbon, gas-phase reaction with first-generation products, or heterogeneous aging of particle-bound dimers), the exocyclic double bond of  $\beta$ -pinene was exploited.  $^{13}C$ - $\beta$ -Pinene, labeled at the terminal vinylic carbon, was synthesized from  $^{13}C$ -iodomethane and nopinone via Wittig olefination (Scheme 1). Ozonolysis of  $^{13}C$ - $\beta$ -pinene was carried out in the CPOT in the absence of an OH scavenger; SOA samples were collected on Teflon filters and extracted into  $H_2O$ . The  $m/z$  of 18 of the identified dimers (Table 1, types 1–3), including the four major BPI peaks, shifted by one mass unit on formation from  $^{13}C$ - $\beta$ -pinene, indicative of  $^{13}C$  incorporation, while their RT remained unchanged. Recalling that reaction of  $^{13}C$ - $\beta$ -pinene with  $O_3$  will cleave the  $^{13}C$  label whereas on reaction with OH the label will be retained, the one-unit mass shift suggests that formation of the 18 dimers occurs via reaction, in either the gas or particle phase, of  $O_3$ -derived products/intermediates with products/intermediates generated from oxidation of  $\beta$ -pinene by OH produced via VHP decomposition. For those dimers that did not undergo a mass shift (Table 1, type 4), the observed dependence of their formation on OH can be rationalized, in addition to the scenarios above, in terms of a photooxidative pathway in which the labeled carbon is

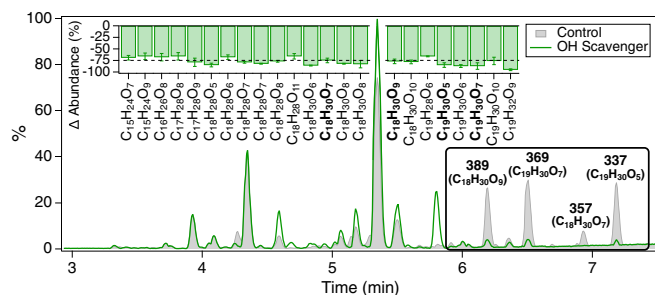


**Fig. 2.** UPLC(–)ESI-Q-TOF-MS BPI chromatograms of SOA produced from the  $O_3$ -initiated oxidation of  $\beta$ -pinene in the CPOT in the presence and absence of cyclohexane as an OH scavenger (*SI Appendix, Table S1*, Exps. 7 and 8). Numbers correspond to nominal  $m/z$  values of  $[M-H]^-$  ions; molecular formulas are given in parentheses. (*Inset*) Dimers that exhibited a significant decrease in abundance due to cyclohexane addition (Table 1), reported as a percent change relative to the control experiment and precise to  $<10\%$ . Data for Control and OH Scavenger experiments are normalized to the total organic carbon content of the corresponding SOA samples (*SI Appendix, S3.4*) and are reported as averages of replicates ( $n = 3$ ).

**Table 1. Dimers identified in SOA produced from the O<sub>3</sub>-initiated oxidation of β-pinene that exhibited a significant decrease in abundance (>65%) due to OH scavenging**

Dimer type	Observed <i>m/z</i> (–)	RT, min	Molecular formula	Error, ppm	O:C	$\overline{\text{O}}\text{S}_\text{C}^\dagger$	$\log\text{C}^*, \mu\text{g m}^{-3}$	Exchangeable hydrogens	SOA mass fraction, <sup>§,¶</sup> %	
1	323.1860	6.86	C <sub>18</sub> H <sub>28</sub> O <sub>5</sub>	0.6	0.28	–1.00	–3.9	2	0.04–0.17	
	355.1754	6.24	C <sub>18</sub> H <sub>28</sub> O <sub>7</sub>	–0.8	0.39	–0.78	–7.6	4	0.11–0.36	
	419.1525	4.70	C <sub>18</sub> H <sub>28</sub> O <sub>11</sub>	–6.7	0.61	–0.33	–15.2	4	0.02–0.16	
	373.1851	5.99	C <sub>18</sub> H <sub>30</sub> O <sub>8</sub>	–2.9	0.44	–0.78	–9.4	4	0.07–0.23	
	405.1764	4.49	C <sub>18</sub> H <sub>30</sub> O <sub>10</sub>	0.7	0.56	–0.56	–13.2	5	0.06–0.62	
	351.1828	5.73	C <sub>19</sub> H <sub>28</sub> O <sub>6</sub>	5.7	0.32	–0.84	–6.1	2	0.10–0.41	
	337.2027	7.16	C <sub>19</sub> H <sub>30</sub> O <sub>5</sub>	3.6	0.26	–1.05	–4.3	2	0.46–2.01	
	369.1916	6.48	C <sub>19</sub> H <sub>30</sub> O <sub>7</sub>	0.8	0.37	–0.84	–7.9	4	2.23–9.24	
	2	341.1960	6.87	C <sub>18</sub> H <sub>30</sub> O <sub>6</sub>	–1.2	0.33	–1.00	–5.7	2	0.06–0.24
		357.1919	6.91	C <sub>18</sub> H <sub>30</sub> O <sub>7</sub>	1.7	0.39	–0.89	–7.6	3	0.39–1.60
373.1851		5.70	C <sub>18</sub> H <sub>30</sub> O <sub>8</sub>	–2.9	0.44	–0.78	–9.4	3	0.14–0.47	
389.1814		6.18	C <sub>18</sub> H <sub>30</sub> O <sub>9</sub>	0.8	0.50	–0.67	–11.3	3	1.88–7.81	
353.1961		6.15	C <sub>19</sub> H <sub>30</sub> O <sub>6</sub>	–0.8	0.32	–0.95	–6.1	3	0.14–0.60	
3	315.1448	5.83	C <sub>15</sub> H <sub>24</sub> O <sub>7</sub>	1.3	0.47	–0.67	–6.6	3	0.02–0.10	
	347.1346	5.19	C <sub>15</sub> H <sub>24</sub> O <sub>9</sub>	1.2	0.60	–0.40	–10.5	3	0.03–0.25	
	375.1653	6.24	C <sub>17</sub> H <sub>28</sub> O <sub>9</sub>	–0.5	0.53	–0.59	–11.0	3	0.02–0.24	
	417.1769	6.76	C <sub>19</sub> H <sub>30</sub> O <sub>10</sub>	1.9	0.53	–0.53	–13.5	2	0.06–0.62	
	403.1963	6.28	C <sub>19</sub> H <sub>32</sub> O <sub>9</sub>	–1.2	0.48	–0.74	–11.6	3	0.07–0.24	
4	345.1549	5.36	C <sub>16</sub> H <sub>26</sub> O <sub>8</sub>	0.1	0.50	–0.63	–8.8	2	0.05–0.50	
	359.1714	5.89	C <sub>17</sub> H <sub>28</sub> O <sub>8</sub>	2.2	0.47	–0.71	–9.1	3	0.32–1.07	
	339.1822	6.34	C <sub>18</sub> H <sub>28</sub> O <sub>6</sub>	4.1	0.33	–0.89	–5.7	2	0.46–1.93	
	355.1754	5.27	C <sub>18</sub> H <sub>28</sub> O <sub>7</sub>	–0.8	0.39	–0.78	–7.6	5	0.51–1.72	
	371.1707	5.46	C <sub>18</sub> H <sub>28</sub> O <sub>8</sub>	0.3	0.44	–0.67	–9.4	3	0.30–1.22	

Dimers are grouped into four types based on structure and formation mechanism (see main text).

<sup>†</sup>Average carbon oxidation state ( $\overline{\text{O}}\text{S}_\text{C} = 2 \text{ O:C} - \text{H:C}$ ).

<sup>‡</sup>Saturation mass concentration (C\*). Estimated using empirical model developed by Donahue et al. (35).

<sup>§</sup>Calculated for β-pinene SOA produced from O<sub>3</sub>-initiated oxidation in the CTEC (SI Appendix, Table S1, Exp. 1) after ~4 h of reaction.

<sup>¶</sup>Upper and lower bounds represent mass fraction estimates derived from experimental and computational approaches, respectively. Uncertainties in experimental and computational approaches are estimated to be ±23% (relative) and a factor of 3, respectively. Details are provided in SI Appendix, S7.

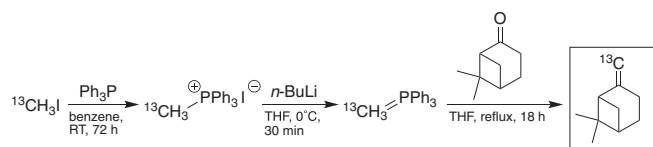
eliminated following OH addition to β-pinene (36, 37) but prior to reaction with the O<sub>3</sub>-derived species.

The steady-state CPOT experiments enabled collection of sufficient quantities of SOA mass for detailed structural analysis via collision-induced dissociation (CID) (SI Appendix, S3.5). MS/MS spectra of the <sup>13</sup>C-labeled dimers and their <sup>12</sup>C isotopologues revealed distinct OH-derived (<sup>13</sup>C-mass-shifted) and O<sub>3</sub>-derived (unshifted) fragmentation patterns (SI Appendix, Table S3). A group of eight dimeric compounds (Table 1, type 1) was identified with fragmentation patterns and relative peak intensities characteristic of covalent dimer esters, which have been reported to be significant components of monoterpene SOA (7, 10–13, 18–21). Specifically, (i) the elemental composition of the dimers is given by condensation of the O<sub>3</sub>- and OH-derived monomeric product ions ( $M_1 + M_2 - M_{\text{H}_2\text{O}} = M_{\text{D}}$ ) (7, 16), and (ii) assuming that the principal fragmentation occurs at the ester linkage, producing carboxyl and alkoxy fragment ions through neutral loss of the alcohol and dehydrated acid moieties, respectively, the carboxyl fragments and associated daughter ions are more intense than the alkoxy fragments and their daughter ions (Fig. 3) (20, 21, 38), in line with conventional charge accommodation behavior in (–)ESI-MS. For the remaining 10 dimers (Table 1, types 2 and 3), the O<sub>3</sub>- and OH-derived fragmentation patterns were not indicative of known accretion chemistry (e.g., formal addition or condensation), and in most instances a reasonable OH-derived (<sup>13</sup>C-mass-shifted) monomeric building block either could not be identified or failed to account for the observed OH-derived daughter ions (SI Appendix, Table S3). The structures of these dimers were not investigated further.

Based on comparison with MS/MS data for commercial standards and/or previously published MS/MS spectra, the O<sub>3</sub>-derived monomeric building blocks of the dimer esters are attributed to one of three dicarboxylic acids, each a well-characterized pinene oxidation product that has been implicated

in dimer formation: *cis*-pinic acid (C<sub>9</sub>H<sub>14</sub>O<sub>4</sub>; Fig. 3A), *cis*-norpinic acid (C<sub>8</sub>H<sub>12</sub>O<sub>4</sub>; Fig. 3B), and diaterpenylic acid (C<sub>8</sub>H<sub>14</sub>O<sub>5</sub>; Fig. 3C) (7, 39) (SI Appendix, S6.1). Conversely, the OH-derived monomeric units are characterized by the ionic [M–H]<sup>–</sup> formulas [C<sub>10</sub>H<sub>15,17</sub>O<sub>2–7</sub>]<sup>–</sup>, indicative of OH addition to β-pinene (C<sub>10</sub>H<sub>16</sub>) followed by varying degrees of O<sub>2</sub> incorporation, isomerization, and bimolecular radical chemistry (36, 37). The daughter ions of the dicarboxylic acid and [C<sub>10</sub>H<sub>15,17</sub>O<sub>2–7</sub>]<sup>–</sup> monomeric units are rationalized by successive neutral losses of H<sub>2</sub>O (18 Da), CO<sub>2</sub> (44 Da), CH<sub>2</sub>O (30 Da), and C<sub>3</sub>H<sub>6</sub>O (58 Da), all of which are established CID pathways (40–42). Notably, the loss of <sup>13</sup>CH<sub>2</sub>O (31 Da) from the [C<sub>10</sub>H<sub>15,17</sub>O<sub>2–7</sub>]<sup>–</sup> fragment is observed in the MS/MS spectrum of almost every <sup>13</sup>C-labeled dimer ester (Fig. 3 and SI Appendix, Table S3), consistent with the expected major addition of OH to β-pinene (83% of total OH reactivity) at the terminal vinylic carbon (36). Moreover, while the three dicarboxylic acids implicated as O<sub>3</sub>-derived precursors were identified as major products in β-pinene SOA formed from ozonolysis (SI Appendix, S6.1), SOA products corresponding to the OH-derived monomeric building blocks (i.e., C<sub>10</sub>H<sub>16</sub>O<sub>3,7</sub> and C<sub>10</sub>H<sub>18</sub>O<sub>2,4,6</sub>) were not detected.

To further constrain the structures of the dimer esters, β-pinene SOA filters were extracted into D<sub>2</sub>O and analyzed via UPLC/(–)ESI-Q-TOF-MS using D<sub>2</sub>O as the polar eluent (SI Appendix,



**Scheme 1.** Synthesis of <sup>13</sup>C-β-pinene via Wittig olefination (SI Appendix, S5).

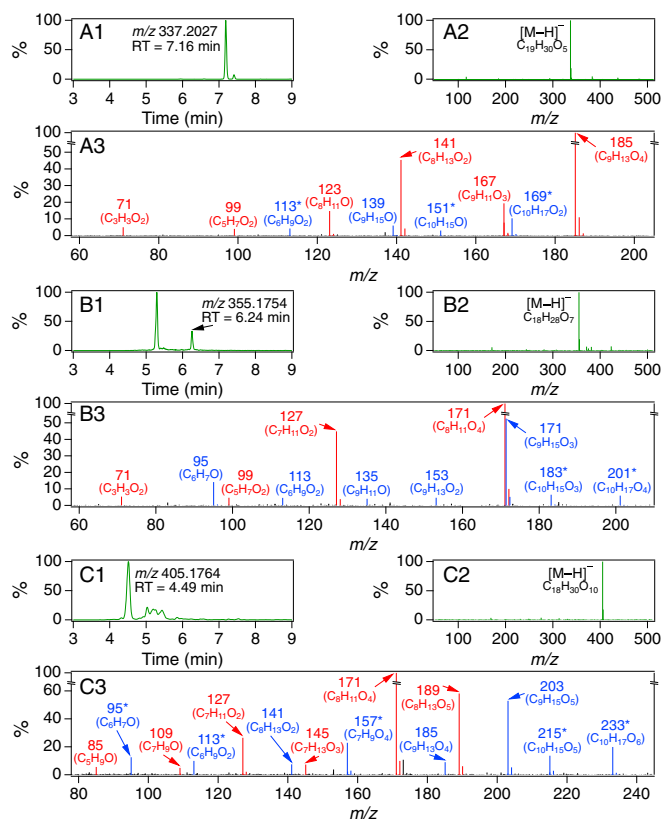


**Fig. 3.** Representative (1) extracted ion chromatograms, (2) MS spectra, and (3) MS/MS spectra, measured by UPLC(–)ESI-Q-TOF-MS, of dimer esters in SOA produced from the  $O_3$ -initiated oxidation of  $\beta$ -pinene (Table 1, type 1) presumed to form from (A) *cis*-pinic acid ( $C_9H_{14}O_4$ ), (B) *cis*-norpinic acid ( $C_8H_{12}O_4$ ), and (C) diaterpenylic acid ( $C_8H_{14}O_5$ ). MS/MS peaks are colored to denote  $O_3$ -derived (red) and OH-derived (blue) fragment ions. Numbers in MS/MS spectra correspond to nominal  $m/z$  values of  $[M-H]^-$  fragment ions; ionic formulas  $[C_xH_yO_z]^-$  are given in parentheses. \*Indicates peaks that underwent a one-unit mass shift on formation from  $^{13}C$ - $\beta$ -pinene.

S3.6). This approach facilitated deuterium substitution ( $H \rightarrow D$ ) of labile hydrogens (e.g.,  $-OH$ ,  $-OOH$ , and  $-COOH$ ) in the SOA constituents while preserving chromatographic separation, enabling quantification of the number of exchangeable hydrogens in the identified dimer molecules based on systematic shifts in  $m/z$  due to H/D exchange (Table 1 and *SI Appendix*, Fig. S4). Additionally, using our recently developed iodometry-assisted LC/ESI-MS assay for the molecular-level identification of organic peroxides (30), it was established that the 23 identified dimers do not contain hydroperoxide (ROOH) or organic peroxide (ROOR) functionalities (*SI Appendix*, S3.7). On the basis of these supporting experiments, the accurate mass (MS) and fragmentation (MS/MS) data, the inferred dicarboxylic acid structures of the  $O_3$ -derived monomers, and the prevailing mechanism of  $\beta$ -pinene photooxidation (36, 37), tentative molecular structures and fragmentation pathways for the dimer esters are proposed in *SI Appendix*, Table S4 and Fig. S10, respectively (*SI Appendix*, S6.1).

**Mechanisms of Dimer Formation.** To assess the relative contributions of gas- vs. particle-phase chemistry to the formation of dimers derived from concerted  $O_3$  and OH oxidation, the temporal evolution of individual products in  $\beta$ -pinene SOA formed from ozonolysis in the CTEC was examined. Shown in Fig. 4A–C are the particle-phase growth profiles of the eight dimer esters (Table 1, type 1) overlaid upon those corresponding to the dicarboxylic acid monomers (*cis*-pinic acid, *cis*-norpinic acid, and diaterpenylic acid) that were implicated as precursors based on detailed MS/MS analysis. The strong correlation between the

particle-phase abundances of the dimer esters and their presumed dicarboxylic acid building blocks points toward a mechanism of heterogeneous formation, wherein the semivolatile dicarboxylic acids undergo traditional equilibrium gas-particle partitioning (43) with subsequent reactive uptake of the gas-phase, OH-derived monomers/intermediates on collision with particle surfaces to form ELVOC dimers. A heterogeneous rather than purely particle-phase mechanism is supported by the absence of monomers corresponding to the OH-derived dimer ester precursors in SOA generated from  $\beta$ -pinene ozonolysis. Such heterogeneous/multiphase accretion processes, leading to the production of high-molecular-weight oligomeric products, have recently been shown to contribute significantly to SOA formation in both biogenic and anthropogenic systems (44, 45).

The growth dynamics of the dimer esters can be contrasted against those shown in Fig. 4D for another group of dimers (Table 1, type 2) also produced from coupled  $O_3$  and OH oxidation. These dimers achieve essentially their maximum, steady-state SOA concentrations after  $\sim 2$  h of reaction, whereas within the same time frame the dimer esters reach only  $\sim 60\%$  of their highest measured particle-phase abundances. Prompt formation and rapid particle-phase growth of the dimers in Fig. 4D, at rates faster than those observed for the monomers (Fig. 4A–C), indicate production via gas-phase reactions of first-generation oxidation products/intermediates followed by irreversible condensation of the resulting ELVOC dimers onto existing aerosol surfaces. As the formation of these dimers was not significantly inhibited by introduction of SCI scavengers (*SI Appendix*, Fig. S1), they likely originate from closed-shell/radical species unique to the hot Criegee VHP channel. Although the identified dimers were found not to contain (hydro)peroxide functionalities (*SI Appendix*, S3.7), production of the dimers in Fig. 4D may be explained by gas-phase  $RO_2$  self/cross-reactions (23–26, 46) with subsequent particle-phase decomposition leading to nonperoxide species (13, 20). Fast formation of particle-bound dimers during monoterpene ozonolysis has been reported in several recent studies (10–13, 20) and, together with their estimated low volatility, has been advanced to explain nucleation and initial growth of monoterpene SOA, both in laboratory studies without seed aerosol and in regions, such as the boreal forest, dominated by biogenic emissions (47).

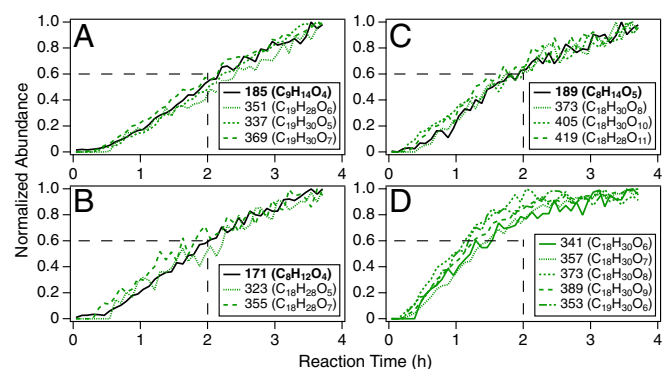


**Fig. 4.** Temporal profiles of molecular products in SOA produced from the  $O_3$ -initiated oxidation of  $\beta$ -pinene in the CTEC (*SI Appendix*, Table S1, Exp. 1), measured by PILS + UPLC(–)ESI-Q-TOF-MS. Profiles are plotted as the particle-phase abundance of each species, normalized to the highest abundance observed over 4 h of reaction, as a function of reaction time. Discrete data points (5-min resolution) are presented as lines to aid the eye. Numbers correspond to nominal  $m/z$  values of  $[M-H]^-$  ions; molecular formulas are given in parentheses. (A–C) Profiles of dimer esters (Table 1, type 1) and dicarboxylic acids implicated as precursors based on MS/MS analysis: (A) *cis*-pinic acid ( $m/z$  185;  $C_9H_{14}O_4$ ; RT 4.33), (B) *cis*-norpinic acid ( $m/z$  171;  $C_8H_{12}O_4$ ; RT 4.06), and (C) diaterpenylic acid ( $m/z$  189;  $C_8H_{14}O_5$ ; RT 3.32). (D) Profiles of dimers (Table 1, type 2) characterized by almost immediate formation and rapid particle-phase growth. Dashed lines (2 h, 0.6 abundance) are drawn to aid in comparison between growth profiles in A–C and D.

As a means of evaluating the hypothesized mechanism of heterogeneous dimer ester formation,  $\beta$ -pinene photooxidation experiments were conducted in the CTEC in the presence of seed aerosol composed of varying mass ratios of ammonium sulfate  $[(\text{NH}_4)_2\text{SO}_4]$  and *cis*-pinic acid, the only commercially available pinene-derived dicarboxylic acid (*Materials and Methods*). Consistent with the idea that introducing the  $\text{O}_3$ -derived dimer ester precursors into the particle phase of the OH system should promote otherwise negligible heterogeneous dimerization, the presence of *cis*-pinic acid in the  $(\text{NH}_4)_2\text{SO}_4$  seed resulted in significant formation, proportional to the mass ratio of *cis*-pinic acid to  $(\text{NH}_4)_2\text{SO}_4$ , of the major dimer ester at  $m/z$  337 ( $\text{C}_{19}\text{H}_{30}\text{O}_5$ ) (Fig. 5), corroborating the indirect MS/MS (Fig. 3A) and kinetic (Fig. 4A) evidence for production from particle-bound *cis*-pinic acid. That the dimer ester at  $m/z$  337 was not observed in OH-derived  $\beta$ -pinene SOA, with pure  $(\text{NH}_4)_2\text{SO}_4$  seed, collected on a Teflon filter coated with *cis*-pinic acid excludes the possibility of dimer formation via accretion of condensed monomers, either on the filter or during the extraction process (*SI Appendix, Fig. S11*). Although the details of the mechanism forming the ester linkage remain unclear, the observed increase in dimer ester abundance at elevated RH (*SI Appendix, Fig. S1*) argues against production via conventional esterification (i.e., carboxylic acid + alcohol). Overall, these findings conclusively demonstrate the role of heterogeneous accretion chemistry in monoterpene SOA formation (*SI Appendix, S6.2*).

Surprisingly, these experiments also imply that a simple mass limitation of monomeric precursors in the particle phase is responsible for the absence of dimer esters in  $\beta$ -pinene SOA formed from OH-initiated oxidation. However, increased mass fractions of *cis*-pinic acid in SOA from  $\alpha$ -pinene ozonolysis, relative to photooxidation, have been observed in a number of previous studies and have been invoked as a possible explanation for the lack of dimers containing *cis*-pinic acid in  $\alpha$ -pinene photooxidation experiments (7, 12, 48). Indeed, in this study *cis*-pinic acid was found to comprise a much higher fraction of  $\beta$ -pinene SOA mass when formed from  $\text{O}_3$ - ( $13.4 \pm 3.1\%$ ) rather than OH-initiated ( $1.7 \pm 0.4\%$ ) oxidation (see  $m/z$  185; RT 4.33 in Fig. 1), while significant but less pronounced disparities in SOA mass fraction between ozonolysis and photooxidation experiments were observed for *cis*-norpinic acid ( $1.4 \pm 0.3\%$  vs.  $0.24 \pm 0.06\%$ ) and diaterpenylic acid ( $0.71 \pm 0.16\%$  vs.  $0.28 \pm 0.06\%$ ) (*SI Appendix, S7*).

Although also suggested to arise from heterogeneous reaction of particle-phase *cis*-pinic acid (Fig. 4A), neither the prominent dimer ester at  $m/z$  369 ( $\text{C}_{19}\text{H}_{30}\text{O}_7$ ) nor the minor dimer ester at  $m/z$  351 ( $\text{C}_{19}\text{H}_{28}\text{O}_6$ ) was detected in the photooxidation experiments carried out with *cis*-pinic acid and  $(\text{NH}_4)_2\text{SO}_4$  seed. One plausible explanation for the absence of these dimers is that the high  $\text{HO}_2$  concentrations ( $\sim 10^{10}$  molecules  $\text{cm}^{-3}$ ) inherent in the use of  $\text{H}_2\text{O}_2$  as an OH precursor (*SI Appendix, S1.1*) produce an

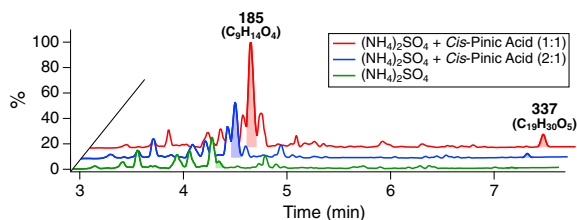


**Fig. 5.** UPLC(-)ESI-Q-TOF-MS BPI chromatograms of SOA produced from the OH-initiated oxidation of  $\beta$ -pinene after  $\sim 4$  h of reaction in the CTEC (*SI Appendix, Table S1*, Exps. 2–4). Experiments were conducted in the presence of seed aerosol at similar mass loadings but different mass ratios (see legend) of  $(\text{NH}_4)_2\text{SO}_4$  and *cis*-pinic acid ( $\text{C}_9\text{H}_{14}\text{O}_4$ ). Numbers correspond to nominal  $m/z$  values of  $[\text{M}-\text{H}]^-$  ions; molecular formulas are given in parentheses. Shaded peaks correspond to *cis*-pinic acid and the dimer ester at  $m/z$  337 ( $\text{C}_{19}\text{H}_{30}\text{O}_5$ ). Chromatograms for each experiment are normalized to the area of the peak at RT 3.93 ( $m/z$  171;  $\text{C}_8\text{H}_{12}\text{O}_4$ ).

oxidative environment in which the OH-derived  $\text{RO}_2$  isomerization and bimolecular reaction channels are vastly different from those operative in the comparatively low- $\text{HO}_2$  ( $\sim 10^7$  molecules  $\text{cm}^{-3}$ ) ozonolysis system (*SI Appendix, S4*) that form the  $[\text{C}_{10}\text{H}_{17}\text{O}_4]^-$  and  $[\text{C}_{10}\text{H}_{15}\text{O}_3]^-$  building blocks of the dimer esters at  $m/z$  369 and 351, respectively (*SI Appendix, Table S3*). That  $\text{RO}_2 + \text{HO}_2$  rate coefficients are typically order(s) of magnitude larger than those for  $\text{RO}_2 + \text{RO}_2$  reactions (49) further compounds the disparity between these two  $\text{RO}_2$  regimes. Conversely, for the dimer ester at  $m/z$  337, although the structure of the  $[\text{C}_{10}\text{H}_{17}\text{O}_2]^-$  building block is tentative (*SI Appendix, Fig. S10* and *Table S3*), theoretical studies indicate that this monomer is able to form under both ozonolysis and photooxidation conditions from the  $\text{C}_{10}\text{H}_{17}\text{O}_3$  hydroxy peroxy radical, produced from OH and subsequent  $\text{O}_2$  addition to  $\beta$ -pinene, either via traditional  $\text{RO}_2 + \text{RO}_2$  chemistry or through an OH-recycling pathway in the reaction with  $\text{HO}_2$  (36, 50).

**Atmospheric Implications.** The production of dimeric compounds (Table 1, types 1–3) through concerted  $\text{O}_3$  and OH oxidation accounts for an appreciable, heretofore-unidentified fraction (5.9–25.4%) of the total mass of  $\beta$ -pinene SOA derived from ozonolysis under the conditions employed in this work (Table 1). Although specifically revealed in SOA formation from  $\beta$ -pinene, this reactive pathway represents a potentially significant source of high-molecular-weight ELVOC to the atmosphere that is expected to be broadly applicable to other monoterpenes (*SI Appendix, S8*). Through detailed molecular composition and kinetic analysis, certain dimers are definitively shown to form through heterogeneous processes, while indirect evidence for dimer production via gas-phase routes is also presented. The importance of both gas- and particle-phase reactions to the formation of dimeric SOA constituents demonstrated in the current work underscores the complexity of atmospheric accretion chemistry, as well as the significant shortcomings in scientific understanding that preclude adequate characterization of its impact.

The  $\text{O}_3 + \text{OH}$  reactivity elucidated in  $\beta$ -pinene SOA also highlights the importance of understanding and accounting for the likely role of oxidative synergism in ambient aerosol formation, where SOA precursors are susceptible to concurrent oxidation by  $\text{O}_3$  and OH. At present, SOA formation in atmospheric models is treated as an additive combination of products originating from the isolated oxidation of individual precursors (e.g.,  $\alpha$ -pinene +  $\text{O}_3$  or isoprene + OH). In establishing that oxidants can act in concert to produce extremely low-volatility dimers in nontrivial yields, however, this study suggests that the tendency of current atmospheric models to systematically underpredict ambient SOA mass (1) may be due in part to the fact that discrete SOA formation mechanisms, parameterized by laboratory experiments that typically feature only one oxidant and a single SOA precursor, do not accurately reflect the intricate oxidation pathways at play in the real atmosphere. Revising the chemistry of monoterpene SOA formation in regional air quality and global climate models to account for the role of synergistic oxidation could help to resolve the discrepancy between model predictions and ambient measurements. However, parameterization of this reactivity requires additional work.

## Materials and Methods

$\beta$ -Pinene ozonolysis and photooxidation experiments were carried out in the CTEC and CPOT at ambient temperature ( $\sim 295$  K) and atmospheric pressure ( $\sim 1$  atm), under dry conditions ( $<10\%$  RH), in the presence of  $(\text{NH}_4)_2\text{SO}_4$  seed aerosol, and at mixing ratios of  $\text{NO}_x$  typical of the pristine atmosphere ( $<0.5$  ppb). CTEC experiments were designed to mimic oxidation in ambient air, while those in the CPOT were used to elucidate dimer structures and formation mechanisms. For CTEC experiments with  $\sim 4$ -h duration,  $\beta$ -pinene ( $\sim 120$  ppb) was oxidized by  $\text{O}_3$  ( $\sim 200$  ppb) in the absence of an OH scavenger or OH ( $\sim 2 \times 10^6$  molecules  $\text{cm}^{-3}$ ). Select photooxidation experiments were performed with mixed  $(\text{NH}_4)_2\text{SO}_4$  and *cis*-pinic acid seed. For steady-state CPOT experiments, oxidation of  $\beta$ -pinene ( $\sim 150$  ppb) by  $\text{O}_3$  ( $\sim 1$  ppm) proceeded in the presence and absence of scavengers for both OH (cyclohexane) and SCl<sub>2</sub> (water vapor and formic acid). In certain CPOT experiments,  $^{13}\text{C}$ - $\beta$ -pinene, synthesized from  $^{13}\text{C}$ -iodomethane and nopinone via Wittig olefination

(Scheme 1), was used. Experimental conditions are reported in *SI Appendix, Table S1* and described in detail in *SI Appendix, S1*.

$\beta$ -Pinene mixing ratios were quantified with a gas chromatograph equipped with a flame ionization detector (GC/FID) (*SI Appendix, S2*). Aerosol size distributions and number concentrations were measured with a custom-built scanning mobility particle sizer (SMPS) (*SI Appendix, S3.1*). "Bulk" aerosol chemical composition was quantified with an Aerodyne high-resolution time-of-flight aerosol mass spectrometer (HR-ToF-AMS) (*SI Appendix, S3.2*). The molecular composition of  $\beta$ -pinene SOA collected by PILS during CTEC experiments (*SI Appendix, S3.3*) and on Teflon filters during steady-state CPOT and select CTEC experiments (*SI Appendix, S3.4*) was characterized off-line by UPLC(–)ESI-Q-TOF-MS (*SI Appendix, S3.5*). Certain SOA filter samples were analyzed using D<sub>2</sub>O in place of H<sub>2</sub>O as the extraction solvent/polar eluent (*SI Appendix, S3.6*). Iodometry was coupled to UPLC(–)ESI-Q-TOF-MS (30) to identify organic peroxides at the molecular level in

$\beta$ -pinene SOA (*SI Appendix, S3.7*). The Master Chemical Mechanism version 3.2 (MCMv3.2) (51) was used to simulate the concentration profiles of OH, HO<sub>2</sub>, and RO<sub>2</sub> during  $\beta$ -pinene ozonolysis in the CTEC, as well as the fractions of  $\beta$ -pinene that react with O<sub>3</sub> vs. OH (*SI Appendix, S4*). Mass fractions of individual organic compounds in  $\beta$ -pinene SOA, along with associated uncertainties, were calculated as described in *SI Appendix, S7*.

**ACKNOWLEDGMENTS.** We thank Xuan Zhang, John Crouse, and Paul Wennberg for useful discussions. UPLC(–)ESI-Q-TOF-MS was performed in the Caltech Environmental Analysis Center. This work was supported by National Science Foundation Grants AGS-1523500 and CHE-1508526. R.Z. acknowledges support from a Natural Science and Engineering Research Council of Canada Postdoctoral Fellowship. J.C.H. acknowledges support from the Camille and Henry Dreyfus Postdoctoral Program in Environmental Chemistry.

- Hallquist M, et al. (2009) The formation, properties and impact of secondary organic aerosol: Current and emerging issues. *Atmos Chem Phys* 9:5155–5236.
- Kanakidou M, et al. (2005) Organic aerosol and global climate modelling: A review. *Atmos Chem Phys* 5:1053–1123.
- Jimenez JL, et al. (2009) Evolution of organic aerosols in the atmosphere. *Science* 326:1525–1529.
- Intergovernmental Panel on Climate Change (2013) *Climate Change 2013: The Physical Science Basis*, eds Stocker TF, et al. (Cambridge Univ Press, Cambridge, UK).
- Pope CA, 3rd, Ezzati M, Dockery DW (2009) Fine-particulate air pollution and life expectancy in the United States. *N Engl J Med* 360:376–386.
- Cohen AJ, et al. (2017) Estimates and 25-year trends of the global burden of disease attributable to ambient air pollution: An analysis of data from the Global Burden of Diseases Study 2015. *Lancet* 389:1907–1918.
- Yasmeen F, et al. (2010) Terpenylic acid and related compounds: Precursors for dimers in secondary organic aerosol from the ozonolysis of  $\alpha$ - and  $\beta$ -pinene. *Atmos Chem Phys* 10:9383–9392.
- Kourtchev I, et al. (2016) Enhanced volatile organic compounds emissions and organic aerosol mass increase the oligomer content of atmospheric aerosols. *Sci Rep* 6:35038.
- Mohr C, et al. (2017) Ambient observations of dimers from terpene oxidation in the gas phase: Implications for new particle formation and growth. *Geophys Res Lett* 44:2958–2966.
- Kristensen K, et al. (2013) Formation and occurrence of dimer esters of pinene oxidation products in atmospheric aerosols. *Atmos Chem Phys* 13:3763–3776.
- Kristensen K, et al. (2016) High-molecular weight dimer esters are major products in aerosols from  $\alpha$ -pinene ozonolysis and the boreal forest. *Environ Sci Technol Lett* 3:280–285.
- Kristensen K, et al. (2014) Dimers in  $\alpha$ -pinene secondary organic aerosol: Effect of hydroxyl radical, ozone, relative humidity and aerosol acidity. *Atmos Chem Phys* 14:4201–4218.
- Zhang X, et al. (2015) Formation and evolution of molecular products in  $\alpha$ -pinene secondary organic aerosol. *Proc Natl Acad Sci USA* 112:14168–14173.
- Zhao Y, Wingen LM, Perraud V, Greaves J, Finlayson-Pitts BJ (2015) Role of the reaction of stabilized Criegee intermediates with peroxy radicals in particle formation and growth in air. *Phys Chem Chem Phys* 17:12500–12514.
- Witkowski B, Gierczak T (2014) Early stage composition of SOA produced by  $\alpha$ -pinene/ozone reaction:  $\alpha$ -Acylhydroperoxy aldehydes and acidic dimers. *Atmos Environ* 95:59–70.
- Hall WA, 4th, Johnston MV (2012) Oligomer formation pathways in secondary organic aerosol from MS and MS/MS measurements with high mass accuracy and resolving power. *J Am Soc Mass Spectrom* 23:1097–1108.
- Tolocka MP, et al. (2004) Formation of oligomers in secondary organic aerosol. *Environ Sci Technol* 38:1428–1434.
- Reinhardt A, et al. (2007) Ultrahigh mass resolution and accurate mass measurements as a tool to characterize oligomers in secondary organic aerosols. *Anal Chem* 79:4074–4082.
- Gao Y, Hall WA, Johnston MV (2010) Molecular composition of monoterpene secondary organic aerosol at low mass loading. *Environ Sci Technol* 44:7897–7902.
- Müller L, Reinnig MC, Warnke J, Hoffmann T (2008) Unambiguous identification of esters as oligomers in secondary organic aerosol formed from cyclohexene and cyclohexene/ $\alpha$ -pinene ozonolysis. *Atmos Chem Phys* 8:1423–1433.
- Müller L, Reinnig MC, Hayen H, Hoffmann T (2009) Characterization of oligomeric compounds in secondary organic aerosol using liquid chromatography coupled to electrospray ionization Fourier transform ion cyclotron resonance mass spectrometry. *Rapid Commun Mass Spectrom* 23:971–979.
- Docherty KS, Wu W, Lim YB, Ziemann PJ (2005) Contributions of organic peroxides to secondary aerosol formed from reactions of monoterpenes with O<sub>3</sub>. *Environ Sci Technol* 39:4049–4059.
- Ehn M, et al. (2014) A large source of low-volatility secondary organic aerosol. *Nature* 506:476–479.
- Jokinen T, et al. (2015) Production of extremely low volatile organic compounds from biogenic emissions: Measured yields and atmospheric implications. *Proc Natl Acad Sci USA* 112:7123–7128.
- Kirkby J, et al. (2016) Ion-induced nucleation of pure biogenic particles. *Nature* 533:521–526.
- Tröstl J, et al. (2016) The role of low-volatility organic compounds in initial particle growth in the atmosphere. *Nature* 533:527–531.
- Kidd C, Perraud V, Wingen LM, Finlayson-Pitts BJ (2014) Integrating phase and composition of secondary organic aerosol from the ozonolysis of  $\alpha$ -pinene. *Proc Natl Acad Sci USA* 111:7552–7557.
- Guenther AB, et al. (2012) The Model of Emissions of Gases and Aerosols from Nature version 2.1 (MEGAN2.1): An extended and updated framework for modeling biogenic emissions. *Geosci Model Dev* 5:1471–1492.
- Zhang X, et al. (2016) Time-resolved molecular characterization of organic aerosols by PILS + UPLC/ESI-Q-TOFMS. *Atmos Environ* 130:180–189.
- Zhao R, Kenseth CM, Huang Y, Dalleska NF, Seinfeld JH (2018) Iodometry-assisted liquid chromatography electrospray ionization mass spectrometry for analysis of organic peroxides: An application to atmospheric secondary organic aerosol. *Environ Sci Technol* 52:2108–2117.
- Donahue NM, Drozd GT, Epstein SA, Presto AA, Kroll JH (2011) Adventures in ozoneland: Down the rabbit-hole. *Phys Chem Chem Phys* 13:10848–10857.
- Sipilä M, et al. (2014) Reactivity of stabilized Criegee intermediates (sCIs) from isoprene and monoterpene ozonolysis toward SO<sub>2</sub> and organic acids. *Atmos Chem Phys* 14:12143–12153.
- Drozd GT, Kurtén T, Donahue NM, Lester MI (2017) Unimolecular decay of the dimethyl-substituted Criegee intermediate in alkene ozonolysis: Decay time scales and the importance of tunneling. *J Phys Chem A* 121:6036–6045.
- Nguyen TL, Peeters J, Vereecken L (2009) Theoretical study of the gas-phase ozonolysis of  $\beta$ -pinene (C<sub>10</sub>H<sub>16</sub>). *Phys Chem Chem Phys* 11:5643–5656.
- Donahue NM, Epstein SA, Pandis SN, Robinson AL (2011) A two-dimensional volatility basis set: 1. Organic-aerosol mixing thermodynamics. *Atmos Chem Phys* 11:3303–3318.
- Vereecken L, Peeters J (2012) A theoretical study of the OH-initiated gas-phase oxidation mechanism of  $\beta$ -pinene (C<sub>10</sub>H<sub>16</sub>): First generation products. *Phys Chem Chem Phys* 14:3802–3815.
- Kaminski M, et al. (2017) Investigation of the  $\beta$ -pinene photooxidation by OH in the atmosphere simulation chamber SAPHIR. *Atmos Chem Phys* 17:6631–6650.
- Reinnig MC, Müller L, Warnke J, Hoffmann T (2008) Characterization of selected organic compound classes in secondary organic aerosol from biogenic VOCs by HPLC/MS<sup>n</sup>. *Anal Bioanal Chem* 391:171–182.
- Yasmeen F, et al. (2011) Characterisation of tracers for aging in  $\alpha$ -pinene secondary organic aerosol using liquid chromatography/negative ion electrospray ionisation mass spectrometry. *Environ Chem* 9:236–246.
- Grossert JS, Fancy PD, White RL (2005) Fragmentation pathways of negative ions produced by electrospray ionization of acyclic dicarboxylic acids and derivatives. *Can J Chem* 83:1878–1890.
- Demarque DP, Crotti AE, Vescechi R, Lopes JL, Lopes NP (2016) Fragmentation reactions using electrospray ionization mass spectrometry: An important tool for the structural elucidation and characterization of synthetic and natural products. *Nat Prod Rep* 33:432–455.
- Kingston DG, Hobrock BW, Bursey MM, Bursey JT (1975) Intramolecular hydrogen transfer in mass spectra. III. Rearrangements involving the loss of small neutral molecules. *Chem Rev* 75:693–730.
- Pankow JF (1994) An absorption model of gas-particle partitioning of organic compounds in the atmosphere. *Atmos Environ* 28:185–188.
- Shiraiwa M, et al. (2013) Size distribution dynamics reveal particle-phase chemistry in organic aerosol formation. *Proc Natl Acad Sci USA* 110:11746–11750.
- Barsanti KC, Kroll JH, Thornton JA (2017) Formation of low-volatility organic compounds in the atmosphere: Recent advancements and insights. *J Phys Chem Lett* 8:1503–1511.
- Berndt T, et al. (2018) Accretion product formation from self- and cross-reactions of RO<sub>2</sub> radicals in the atmosphere. *Angew Chem Int Ed Engl* 57:3820–3824.
- Glasius M, Goldstein AH (2016) Recent discoveries and future challenges in atmospheric organic chemistry. *Environ Sci Technol* 50:2754–2764.
- Kourtchev I, et al. (2015) Molecular composition of fresh and aged secondary organic aerosol from a mixture of biogenic volatile compounds: A high-resolution mass spectrometry study. *Atmos Chem Phys* 15:5683–5695.
- Orlando JJ, Tyndall GS (2012) Laboratory studies of organic peroxy radical chemistry: An overview with emphasis on recent issues of atmospheric significance. *Chem Soc Rev* 41:6294–6317.
- Eddingsaas NC, Loza CL, Yee LD, Seinfeld JH, Wennberg PO (2012)  $\alpha$ -pinene photooxidation under controlled chemical conditions—Gas-phase composition in low- and high-NO<sub>x</sub> environments. *Atmos Chem Phys* 12:6489–6504.
- Saunders SM, Jenkin ME, Derwent RG, Pilling MJ (2003) Protocol for the development of the Master Chemical Mechanism MCM v3 (Part A): Tropospheric degradation of non-aromatic volatile organic compounds. *Atmos Chem Phys* 3:161–180.